Materials Research Proceedings 28 (2023) 987-996 https://doi.org/10.21741/9781644902479-108

Modification of the surface integrity of powder metallurgically produced S390 via deep rolling

HERRMANN Peter[1,a], HERRIG Tim[1,b] and BERGS Thomas[1,2,c]

[1]Laboratory for Machine Tools and Production Engineering (WZL) of RWTH Aachen University, Campus-Boulevard 30, 52074 Aachen

[2]Fraunhofer Institute for Production Technology IPT, Steinbachstr. 17, 52074 Aachen

[a]p.herrmann@wzl.rwth-aachen.de, [b]t.herrig@wzl.rwth-aachen.de, [c]t.bergs@wzl.rwth-aachen.de

Keywords: Deep Rolling, Powder-Metallurgical Steel, Surface Integrity, Residual Stress

Abstract. Fine blanking is an economical process for manufacturing sheet metal workpieces with high sheared surface quality. When machining high-strength steels, material fatigue leads to increased punch wear, which reduces the economic efficiency of the process. This fatigue of the cutting edge and lateral punch surface can be counteracted by mechanical surface treatments. Deep rolling has proved particularly useful for such surface modification, as it allows both: machining of the lateral punch surface and the application of the cutting edge rounding required for fine blanking. For the precise design of the fine blanking punch contour especially the macroscopic deformation of the workpiece is decisive. In this paper, the possibility of specifically modifying the surface integrity of hardened and powder metallurgically produced S390 by means of the incremental surface treatment process deep rolling is investigated. By varying the decisive process parameters rolling pressure, ball diameter and step over distance, their influence on surface integrity is determined. The surface integrity is afterwards characterized by macro hardness, surface topography and residual stress state and microstructural images.

Introduction

Due to the limited availability of geo resources, their use has to be made more efficient by reducing demand and by responsible handling. In mechanical engineering, this results in high demands on the functional integration of technical components. From an economic point of view, short and efficient process chains are required, from which the need for fewer and technologically more complex tools derives. Thus, the demand on the dimensional accuracy and the mechanical properties of tools increase [1].

In particular, fine blanking offers a suitable potential for the economical production of functional components with high quality, due to the high sheared surface quality. Fine blanked components often have to withstand significant loads, which is why high-strength materials are increasingly used in fine blanking [2]. The challenge in processing higher-strength materials is to control the increased tool loads [3]. The highest stress is present on the lateral surface of fine blanking punches. This challenge can be met by improving wear resistance of active surfaces of fine blanking punches.

Deep rolling is a promising technology for increasing the service life of alternately loaded fine blanking punches [4]. Deep rolling is an industrially established process that is used to increase the service life of dynamically loaded components [5]. The process principle is based on incremental elastic-plastic deformation of the component edge zone with a hard rolling body. The local forming of the surface-near edge zone leads to a smoothing of the roughness peaks, induction of residual compressive stresses and strain hardening. These edge zone properties have proven a positive effect on the fatigue strength of components [6].

Content from this work may be used under the terms of the Creative Commons Attribution 3.0 license. Any further distribution of this work must maintain attribution to the author(s) and the title of the work, journal citation and DOI. Published under license by Materials Research Forum LLC.

The cause-and-effect relations between the process kinetics in incremental forming processes, such as deep rolling, and the resulting surface integrity are widely known phenomenologically. However, to extend the application field of deep rolling to include the knowledge-based design of deep rolling processes, material-specific knowledge is required. The overall objective of the studies performed is thereby to reduce abrasive wear on fine blanking punches by means of introducing compressive stresses and surface smoothing. For this reason, specific cause-and-effect relations between the process parameters of deep rolling and the surface integrity of powder metallurgically produced S390 high-speed steel are investigated in this work by means of an experimental parameter study. Powder metallurgically produced S390 high-speed steel is a typical material for fine blanking punches that are conventionally hardened and PVD-coated [7].

Materials and Methods

First, the material of the cylindrical hardened S390 specimens is discussed. Then the experimental setup for the deep rolling within a lathe is presented and the experimental plan is explained. Finally, the measurement methods and the parameters obtained are presented.

The cylindrical specimens (diameter d = 49 mm; length l =60 mm) were set to a hardness of 722 HV30 (61.1 HRC) in preparation for the test. The final specimen geometry was then adjusted by grinding. The material used is the powder-metallurgical S390 from BÖHLER (VOESTALPINE BÖHLER EDELSTAHL GMBH & CO KG, Kapfenberg, Austria), which has the chemical composition given in table 1.

Table 1. Chemical Composition of powder-metallurgical S390 in m-% [8].

C	Si	Mn	P	S	Cr	Mo	Ni	V	W	Co	O
1.63	0.30	0.26	0.018	0.018	4.91	2.28	0.20	5.12	10.09	8.32	0.0041

Due to the chemical composition and the powder-metallurgical microstructure, the compressive strength of the material after heat treatment is in the range of 2,800 to 3,900 MPa. At the same time, the material achieves high toughness: with a hardness of up to 68 HRC, bending strengths of over 4,000 MPa are achieved. The material is characterized by a homogeneous microstructure and, in particular, by the alloying elements tungsten and cobalt, by high wear and high-temperature strength. [8]

Deep Rolling Setup.

The practical test was carried out with a hydrodynamic deep rolling tool from ECOROLL (ECOROLL AG, Celle, Germany) on a conventional lathe. Fig. 1 shows a schematic representation of the test setup and the operating principle of the hydrodynamic deep rolling tool. The lubricant and hydraulic fluid for the hydrodynamic deep rolling tool is the machine's lubricant supply.

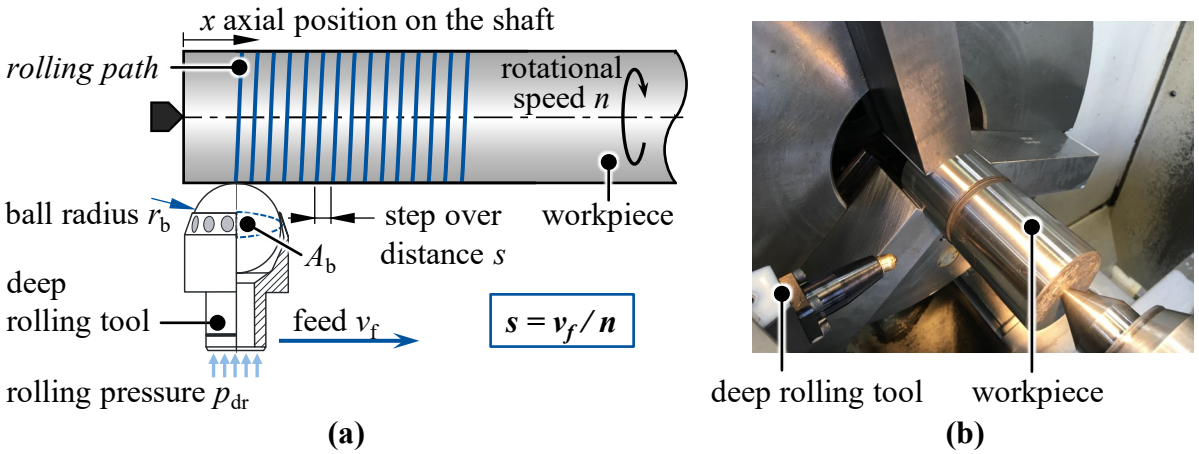

Fig. 1. (a) Test setup including tool and workpiece and properties of the hydrodynamic deep rolling tool from the ECOROLL AG according to [9] and (b) Arrangement of tool and specimen in the lathe.

Fig. 1a shows the schematic test setup. While the workpiece rotates at a constant rotational speed n, the tool moves in axial direction along the workpiece at the feed v_f. From the rotational speed n and feed v_f, the step over distance s results to $s = v_f/n$.

Fig. 1a schematically shows the characteristics of the hydrodynamic deep rolling tool. The rolling ball can be moved dynamically by an infeed during the process. This ensures that the rolling ball and the workpiece are in constant contact during the process. The rolling force F_{dr} is proportional to the rolling pressure p_{dr} and the ball cross-section area A_b and results from the linear relation:

$$F_{dr} = A_b \cdot p_{dr} \cdot (1 - \delta) \text{ with } A_b = d_b^2/4 \cdot \pi. \quad (1)$$

The friction loss δ characterizes the pressure loss between the hydraulic unit and the real pressure applied to the rolling ball. Different loss terms result for different ball diameters d_b and the correspondingly different rolling ball holder:

- $d_b = 3$ mm $\rightarrow \delta_{3mm} = 0.261$
- $d_b = 6$ mm $\rightarrow \delta_{6mm} = 0.236$
- $d_b = 13$ mm $\rightarrow \delta_{13mm} = 0.297$

To determine the friction loss, the rolling force applied at a set pressure was determined for each ball diameter. For this purpose, a test workpiece was fixed on a force measurement platform and the rolling forces for different rolling pressures were determined for each of the three tools ($d_b = 3$ mm, $d_b = 6$ mm and $d_b = 13$ mm). By knowing F_{dr}, p_{dr} and d_{dr}, the friction loss delta could be determined according to Eq. 1, which is specific and constant for each of the three tools.

Test Design.

As a first step it was demonstrated that a significant modification of roughness, hardness and/or residual stress state can be induced by incremental surface treatment. To demonstrate this modification experimentally and to grant a deeper understanding around cause-effect relationships between the deep rolling parameters and the resulting surface integrity, a full factorial experimental design with twofold repetition was used. The process parameters that can be set at the process directly, are the rolling ball diameter d_{dr}, the rolling pressure p_{dr} and step over distance s, which have already been described in the section *Deep Rolling Setup*. The actual parameter values used are shown in Table 2.

Table 2. Parameters of the executed deep rolling experiments.

Deep Rolling Parameter	Parameter Values
Rolling Pressure p_{dr} /MPa	10; 25; 40
Ball diameter d_{dr} /mm	3, 6, 13
Step over distance s /µm	100; 300; 500

In the case of the ECOROLL tool used, the rolling pressure p_{dr} can be varied continuously in the range from 0 to 40 MPa, with this maximum value being fully utilized by the test plan. The step over distances s are selected in such a way that complete machining of the surface is ensured even with the smallest ball impression, but at the same time no excessive machining time occurs. In contrast to the other two parameter variations, the ball diameter d_{dr} increments are not selected equidistantly, since only the three specified diameters are available as tools here. In total, 27 different test setups result from the full-factorial test plan. In the following, the samples are denoted by p_{dr}/MPa-d_{dr}/mm-s/µm (Ex. p_{dr} =10 MPa; d_{dr} = 3 mm; s = 100 µm → 10-3-100).

Measurement methods and objectives.

After the practical test execution, roughness measurements were carried out according to EN ISO 25178. The arithmetical mean height of the surface (S_a) and the maximum height of the surface (S_z) were determined as 3d-surface roughness parameters. To describe the waviness, the value *WDsm* (Mean period length of the dominant waviness) was used in accordance with VDA 2007. These topography measurements were made on a MAHR LD 260 equipped with a MAHR LP C 45-20-5/90° probe (MAHR GMBH, Göttingen, Germany). Furthermore, HV5 and HV30 hardness tests according to Vickers (EN ISO 6507) were carried out. For statistical validation, these test values were recorded five times each. The test values given below are the average of these five values, each of which was measured on a ZWICKROELL ZHU 50 measuring instrument (ZWICKROELL GMBH & CO. KG, Ulm, Germany). In order not to modify the surface condition, the surfaces were specially prepared for the test. The residual stress states presented were analyzed by means of X-ray diffraction using XSTRESS 3000 Mythen (STRESSTECH GMBH, Rennerod, Germany). The depth increments at which the residual stresses were measured are noted at the corresponding position in the diagram.

Results

In order to derive cause-effect relations between the deep rolling parameters and the surface integrity, the smoothing of roughness peaks, the hardness and the residual stress state of the results were investigated. In the following, the results of these investigations are presented and corresponding interactions are derived.

Roughness Measurements. The roughness was reduced with almost all deep rolling setups. The maximum roughness reduction from S_a = 0.44 µm to S_a = 0.21 µm was achieved with a rolling pressure p_{dr} = 40 MPa, ball diameter d_b = 6 mm and step over distance s = 100 µm. On average, S_a was reduced by 27% to 0.32 µm. Fig. 2 shows these influences deep of the rolling parameters on the roughness S_a and additionally on S_z. A measuring point corresponds in each case to the arithmetic mean of the nine corresponding measured values.

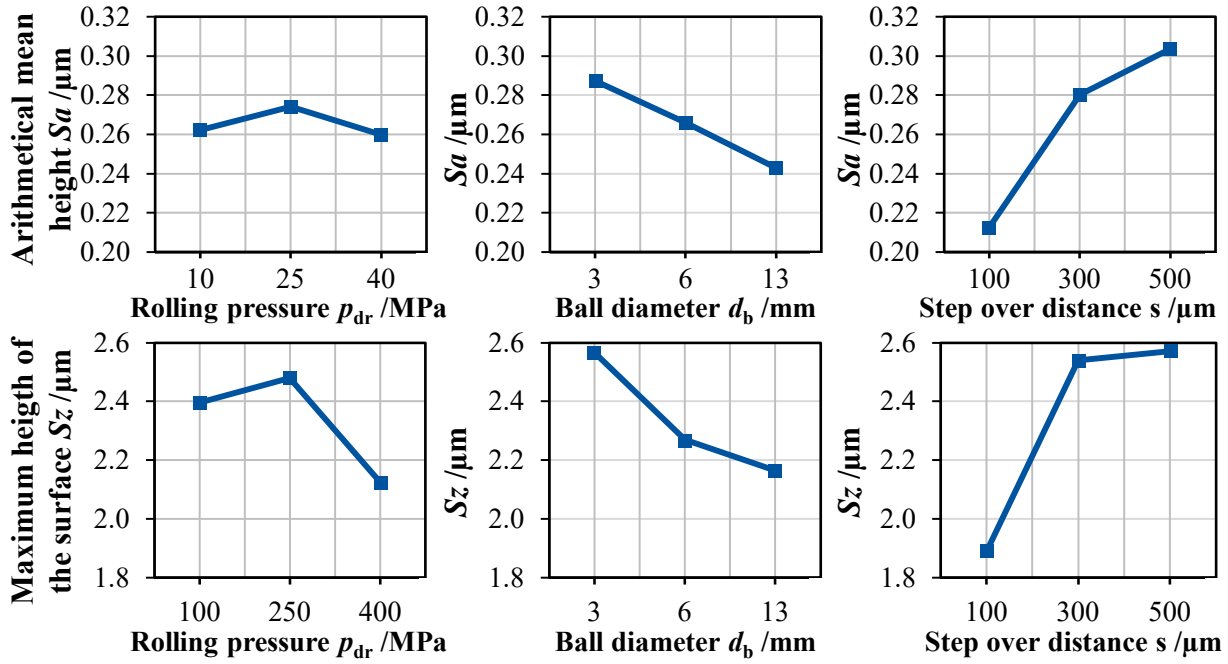

Fig. 2. Main effect plots of the influences of the deep rolling parameters on the arithmetical mean height and the maximum height of the surface.

With respect to S_a, the rolling pressure shows the smallest influence of the three parameters. With increasing rolling pressure p_{dr}, no clear trend in S_a can be identified. There is a clear correlation between the rolling ball diameter d_b and S_a. S_a decreases significantly with increasing d_b. The opposite behavior is found for the dependence on step over distance s. With increasing s, S_a also increases. The results for S_z show similar dependencies as for S_a. With regard to the rolling pressure p_{dr}, no clear trend is established, S_z decreases with increasing ball diameter d_b and increases with larger step over distance s.

In addition to roughness, the waviness of the topography was investigated. In the initial state, the length of the dominant waviness *WDsm* was determined to 0.363 mm. Fig. 3 shows the measured values for *WDsm* for all test setups.

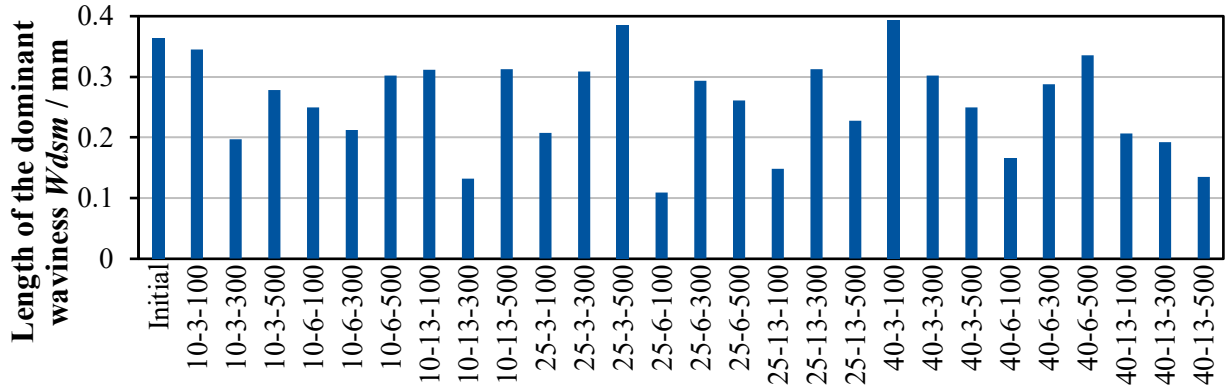

Fig. 3. Length of the dominant waviness Wdsm.

None of the three test parameters shows a correlation with the length of the dominant waviness *WDsm*. In test series carried out with an identical test setup but an initial hardness of 51 HRC, the

selected step over distance *s* and *WDsm* are identical. This expected value is not achieved here. The results rather suggest that there is no correlation between test parameters and *WDsm*.

Hardness tests.

Fig. 4 shows an overall summary of the Vickers hardness tests (HV30). Significant hardness increase was achieved with all deep rolling setups. The maximum hardness increase from 722 HV30 in the initial condition (61.3 HRC) to 882 HV30 (65.7 HRC) was obtained with a rolling pressure p_{dr} = 40 MPa, a ball diameter d_b = 13 mm and a step over distance s = 500 µm. Overall, the hardness values vary in a range of 90 HV30.

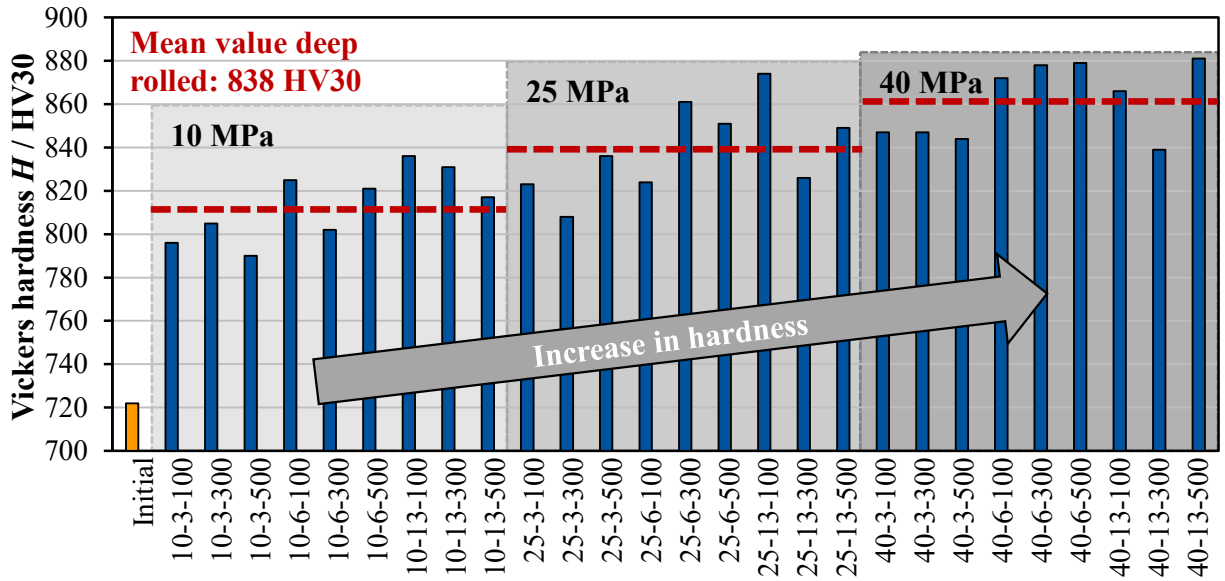

Fig. 4. Overview over the Vickers hardness HV30 for each setup.

On average, a hardness increase of 16% (116 HV30) to 838.6 HV30 was achieved. All hardness values obtained for a rolling pressure p_{dr} = 10 MPa are below this average, whereas all hardness values for p_{dr} = 40 MPa are above this value. The values for p_{dr} = 25 MPa are in between. This tendency can also be seen in the main effect diagrams shown in Fig. 5. The data shown include test values for HV5 as well as HV30. The comparison of the two test forces with each other shows significantly higher HV5 values than HV30 values for a majority of the data points.

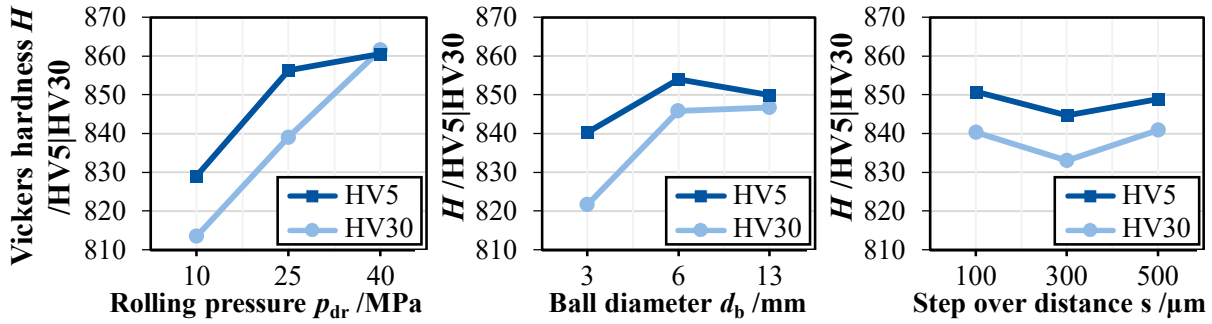

Fig. 5. Main effect plots of the influence of the deep rolling parameters on Vickers hardness HV5 and Vickers hardness HV30.

Due to the lower depth of penetration of the indenter at the low selected test load (HV5), the area of the edge zone closer to the surface has a higher hardness than the edge zone depth covered by the HV30 test. Furthermore, for the HV30 values there is a correlation between the rolling pressure p_{dr} and the Vicker hardness H. H also increases with the rolling ball diameter d_b, although only marginally between d_b = 6 mm and d_b = 13 mm; for the HV5 values this trend is even regressive. In contrast, no clear trend emerges with regard to the step over distance s. Similar hardness values are achieved with all three step over distances s. The test values of H and s do not correlate with each other, which is why s is no longer considered in the following analysis.

In Fig 6. interaction diagrams of the Vickers hardness HV30 as a function of rolling pressure p_{dr} and rolling ball diameter d_b and as a function of d_b and p_{dr} are represented.

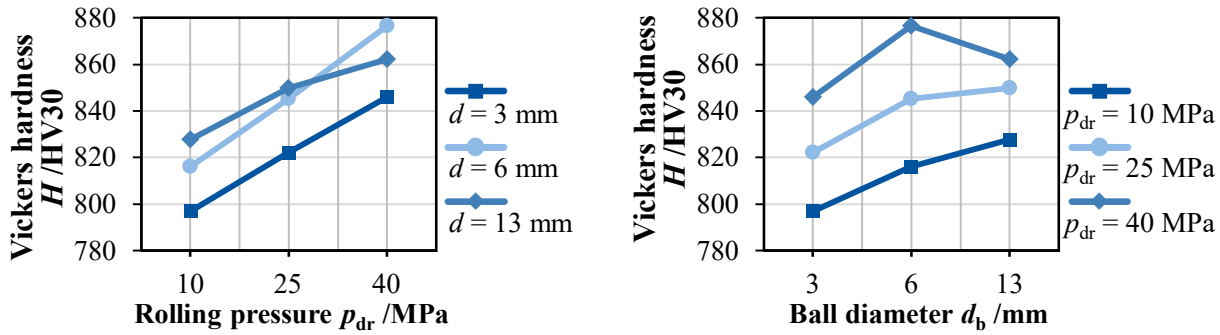

Fig. 6. Interaction diagram of Vickers hardness HV30 as a function of rolling pressure and rolling ball diameter and as a function of rolling ball diameter and rolling pressure.

For each set ball diameter d_b, an increase in rolling pressure is accompanied by a significant increase in hardness. It should be noted that, except for one data point, the largest ball diameter d_b produces the highest hardness at the same pressure. This trend is illustrated in the right hand diagram. The two diagrams show that the differences between the ball diameters of d_b = 6 mm and d_b = 13 mm are comparatively small. The hardness values for d_b = 3 mm are always lower than those of the other two ball diameters at constant pressure. Nevertheless, even with d_b = 3 mm, an increase in hardness can be achieved which is significantly above the hardness value obtained on average.

In contrast to the previous diagrams, in Fig. 7 the Vickers hardness H is not given as a function of one of the three process parameters listed in the test design, but as a function of a resulting variable. The rolling forces F_{dr} given in Fig. 7 are determined according to Eq 1.

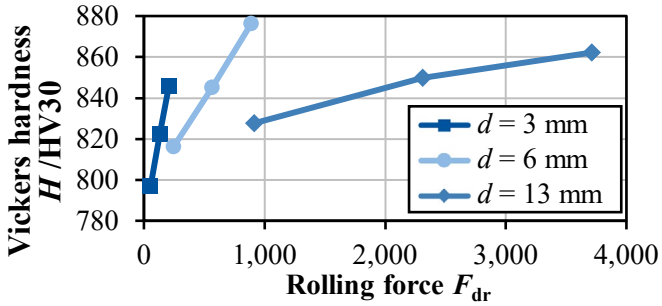

Fig. 7. Interaction diagram of Vickers hardness HV30 as a function of rolling force and rolling ball diameter.

For each of the three ball diameters d_b, the Vickers hardness H correlates with the rolling force F_{dr}. While the smallest hardness increase also occurs at lowest F_{dr} used, the largest hardness values do not occur at $F_{dr,max} \approx 3{,}711$ N but at $F_{dr} \approx 912$ N and the average ball diameter $d_b = 6$ mm. On average, the smallest increases in hardness are obtained with $d_b = 3$ mm and the largest with $d_b = 13$ mm. Nevertheless, even with $d_b = 3$ mm and the comparatively low rolling force $F_{dr} = 208$ N, a hardness increase up to 846 HV30 can be achieved, which is higher than the 839 HV30 achieved on average.

Residual stress analysis.

In addition to the results presented so far, exemplary residual stress curves were measured. All graphs in Fig. 8 show the residual stresses in the axial direction of the specimens, respectively orthogonal to the rolling path. The three graphs show the residual stress curves for the non-deep-rolled initial condition; a rolling pressure $p_{dr} = 40$ MPa, the rolling ball diameter $d_b = 3$ mm and a step over distance s = 500 µm, as well as $p_{dr} = 10$ MPa, $d_b = 3$ mm and $s = 100$ µm.

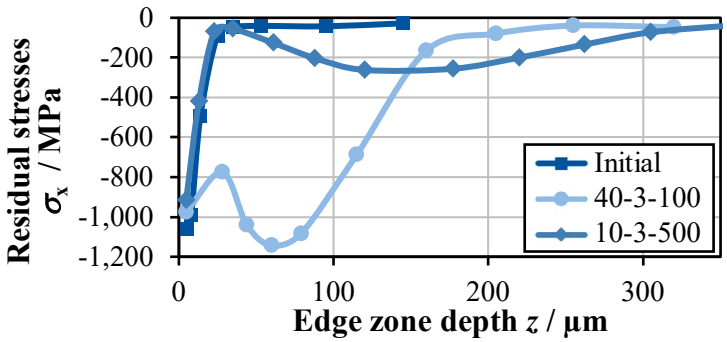

Fig. 8. Depth profile of the residual stress state of selected parameter setups.

In the initial state, a compressive residual stress state is present up to a edge zone depth of $z \approx 25$ µm. At the surface, these residual stresses reach a value of $\sigma_x \approx$ -1,000 MPa. A similar value remains after deep rolling with the rolling pressure $p_{dr} = 10$ MPa. However, here a slight compressive residual stress state is evident at deeper edge zone depths in contrast to the initial condition. For the deep rolling setup with $p_{dr} = 40$ MPa, a similar value of $\sigma_x \approx$ -1,000 MPa is again present at the surface. Here, the maximum residual compressive stresses are, at a depth $z = 60$ µm, at $\sigma_x \approx$ -1,240 MPa. In the range $z > 150$ µm, however, the test setup with lower $p_{dr} = 10$ MPa exhibits greater residual compressive stresses.

Discussion

The surface integrity of powder-metallurgical S390 with an initial hardness of 722 HV30 (61.1 HRC) and an arithmetical height of 0.44 µm can be significantly modified by hydrodynamic deep rolling. With regard to the smoothing of roughness peaks, large rolling ball diameters and a small step over distance have a particularly positive effect. Minimal roughness can be achieved with small rolling ball diameters, but not with large step over distances. Since the influence of rolling pressure on roughness does not show a clear tendency, it can also be assumed that the rolling force, which is proportional to the rolling pressure, has only a subordinate influence in the parameter space considered. It remains unclear to what extent a further reduction in step over distance or larger rolling ball diameters will cause further smoothing.

The results of the waviness analysis show that the spherical ball impression is not introduced into the surface as a distinct path. It is not possible to create a defined path as an impression of the rolling ball at the high initial hardness. Otherwise, the length of the dominant waviness would result directly from the step over distance used. Since this is possible at lower initial hardness, it

can be assumed that the tool is deflected by the material accumulation next to the rolling path that occurs during deep rolling.

The increase in hardness was achieved in particular by using large rolling ball diameters and rolling pressures. A more detailed examination reveals that the rolling ball diameter has only a minor influence, since the maximum hardness increase was not achieved with the largest rolling ball diameter and large hardness increases were achieved independently from the ball diameter. Since neither the rolling pressure nor the rolling force are the main influencing parameters, it can be assumed that the surface pressure present in the contact has a decisive influence.

By comparing HV5 and HV30 test results, it could be shown that the near-surface edge zone achieves a higher hardness than deeper material regions. Furthermore, the HV5 and HV30 test values converge strongly with increasing rolling pressure and increasing rolling ball diameter. This circumstance shows that with increasing rolling pressure and increasing rolling ball diameter, deeper edge zone layers (tested with HV30) reach a similarly high hardness as the near-surface edge zone region (tested with HV5). The work hardening is introduced correspondingly deeper into the workpiece.

Furthermore, it was found that despite the comparatively low rolling force of 208 N, high residual compressive stresses of over 1,100 MPa were introduced into the surface-near edge zone. In contrast to the hardness increase, which was already significant at a rolling force of 52 N, the same parameter setup shows a clear but only slight residual compressive stress introduction. Due to the significantly higher hardness values achieved with a larger rolling ball diameter and greater rolling force, it can be assumed that, with appropriate parameter selection, significantly higher residual compressive stresses will also occur.

Summary

In order to achieve the overall objective of increasing the strength of fine blanking punches with regard to abrasive wear, an experimental study was carried out in this paper. The cause-effect relationships determined are used to design a knowledge-based deep rolling process that increases the service life of fine blanking punches by specifically modifying the surface integrity.

Since it can be assumed that low roughness, high hardness values, and the highest possible near-surface compressive residual stresses lead to high strength, several recommendations can be made for the design of a suitable deep rolling process:

- Minimum roughness can be achieved with any rolling ball diameter. The main parameter influencing the resulting roughness is the step over distance, which should be selected as small as possible.
- High hardness increases can be induced in particular with high rolling pressures. In addition, high rolling pressure causes deeper work hardening.
- Larger rolling ball diameters tend to have a positive effect on hardness, but maximum hardness is not achieved at the largest rolling ball diameter selected. It is assumed that in the process the highest possible surface pressure leads to large increases in hardness.
- Significant residual compressive stresses occur even at low rolling forces. It can also be assumed that higher and deeper residual compressive stresses are produced with greater energy input.

For the design of a fine blanking die, the hardness to which the material is to be set before deep rolling must be taken into account. In addition, a suitable cutting edge rounding must be selected, taking into account the macroscopic deformation caused by deep rolling.

Based on the known phenomenological relationships, it can be assumed that increased strength can be achieved by the shown modifications of the surface integrity. Nevertheless, it remains to provide this evidence experimentally. For this purpose, the possible change in surface integrity due to the subsequent coating process must be determined. Subsequently, practical fine blanking

tests must be carried out on higher-strength sheets in order to provide practical proof of the strength increase.

Funding
This work was funded by the Deutsche Forschungsgemeinschaft (DFG, German Research Foundation) – project number 423492562

References
[1] T. Bergs, M. Wilms, O. Henrichs, S. Weber, G. Stepien, T. Dannen, M. Prümmer, K. Arntz, Individual process chains in toolmaking through data and model-based forecasts, in: Laboratory for Machine Tools and Production Engineering (WZL) of RWTH Aachen University (Ed.), 30th Aachen Machine Tool Colloquium 2021, Aachen, 2021, pp. 80-102.
[2] U. Aravind, U. Chakkingal, P. Venugopal, A Review of Fine Blanking: Influence of Die Design and Process Parameters on Edge Quality, J. Mater. Eng. Perform. 30 (2021) 1-32. https://doi.org/10.1007/s11665-020-05339-y
[3] Y. Abe, T. Kato, K-i, Mori, S. Nishino, Mechanical clinching of ultra-high strength steel sheets and strength of joints, J. Mater. Process. Technol. 214 (2014) 2112–2118. https://doi.org/10.1016/j.jmatprotec.2014.03.003
[4] M. Krobath, T. Klünsner, W. Ecker, M. Deller, N. Leitner, S. Marsoner, Tensile stresses in fine blanking tools and their relevance to tool fracture behavior, Int. J. Machine Tool. Manuf. 126 (2018) 44–50. https://doi.org/10.1016/j.ijmachtools.2017.12.005
[5] D. Meyer, J. Kämmler, Surface Integrity of AISI 4140 After Deep Rolling with Varied External and Internal Loads, Procedia CIRP 45 (2016) 363-366. https://doi.org/10.1016/j.procir.2016.02.356
[6] X. Wang, X. Xiong, K. Huang, S. Ying, M. Tang, X. Qu, W. Ji, C. Qian, Z. Cai, Effects of Deep Rolling on the Microstructure Modification and Fatigue Life of 35Cr2Ni4MoA Bolt Threads, Metals 12 (2022) 1224. https://doi.org/10.3390/met12071224
[7] K. Bobzin, C. Kalscheuer, M. Carlet, D.C. Hoffmann, T. Bergs, L. Uhlmann, Low-Temperature Physical Vapor Deposition TiAlCrSiN Coated High-Speed Steel: Comparison Between Shot-Peened and Polished Substrate Condition, Adv. Eng. Mater. 24 (2022) 2200099. https://doi.org/10.1002/adem.202200099
[8] voestalpine Böhler Edelstahl GmbH & Co. KG, S390 DE: Microclean, Karpfenberg, 2010.
[9] F. Klocke, Fertigungsverfahren 4, Springer Berlin Heidelberg, Berlin, Heidelberg, 2017.